Energy-Efficient Machining Process Analysis and Optimisation Based on BS EN24T Alloy Steel as Case Studies

Caires Moreira, L., Li, W., Lu, X. & Fitzpatrick, M.

DOI 10.1016/j.rcim.2019.01.011
ISSN 0736-5845
ESSN 1879-2537

Publisher: Elsevier

Energy-Efficient Machining Process: Qualitative Analysis and Optimisation

L.C. Moreira, W.D. Li, X. Lu, M.E. Fitzpatrick
Faculty of Engineering, Environment and Computing, Coventry University, Priory Street, Coventry CV1 5FB, United Kingdom

Abstract

Computer Numerical Controlled (CNC) machining is one of the most widely-deployed manufacturing processes. It is important to develop energy-efficient CNC machining processes to achieve the overall goal of sustainable manufacturing. Due to the complexity of machining parameters, it is challenging to develop effective modelling and optimisation approaches to implement energy-efficient CNC machining. In this paper, via experiments and qualitative analysis, the impact that key machining parameters have on energy consumption of milling processes on BS EN24T alloy (AISI 4340) has been investigated in detail. A multi-objective optimisation model has been formulated, and a novel improved multi-swarm Fruit Fly optimisation algorithm (iMFOA) has been developed to identify optimal solutions. Case studies and algorithm benchmarking have been conducted to validate the effectiveness of the optimisation approach. The relationships between energy consumption and key machining parameters (e.g., cutting speed, feed per tooth, engagement depth) have been analysed to support process planners in implementing energy saving measures efficiently. The optimisation approach developed is effective in fine-tuning the key parameters for enhancing energy efficiency while meeting other production technical requirements.

Keywords: CNC machining, optimisation, sustainable manufacturing

1. INTRODUCTION

Ambitious goals to achieve significant energy savings have been set by major economies such as Europe, China and the USA. The manufacturing sector is a major consumer of energy and critical raw materials. Therefore, it is vital to develop effective sustainable manufacturing approaches to achieve the targets of energy savings for global societies. Within the manufacturing sector, Computer Numerical Controlled (CNC) machining is one of the major processes. For CNC machining, process planning is a significant decision-making stage to determine the quality and productivity of machining. In addition, according to [1], process planning is increasingly concerned with reducing energy consumption of machining processes. The exponential growth in research publications related to process planning for energy-efficient CNC machining, which has been recently summarised by Moreira *et al.* [2], demonstrates the importance of this topic worldwide.

Energy information from machining process is the key to assist process planning or lifecycle analysis and improve energy efficiency [3]. Furthermore, it is crucial to develop effective energy consumption modelling and optimisation methodologies to support process planning in implementing energy-efficient machining. CNC machining processes are complex in terms of various cutting parameters, machining strategies and operations, which decision-making for process planning are overwhelming human capabilities. It is important to develop an effective optimisation solution, by creating knowledge-embedded soft computing methods, to assist humans in planning more efficient processes. To-date, some energy consumption optimisation approaches for process planning for CNC machining have been developed [4]. To address the current research gaps, this paper presents qualitative analysis and optimisation considering key machining parameters for CNC processes to achieve energy efficient processes.

In this paper, experimental investigation on the relationship between key machining parameters and energy consumption has been conducted. This facilitates machining process planners to choose suitable cutting parameters to minimise energy consumption during machining. A multi-objective optimisation model has been formulated, considering the energy efficiency, productivity and cutting tool life to fine-tune machining parameters. An improved multi-swarm fruit fly optimisation algorithm (iMFOA) has been developed for solving the optimisation problem. Case studies and algorithm benchmarking have been conducted to validate the effectiveness of the algorithm.

2. BACKGROUND

2.1 Energy consumption modelling

Rising energy costs and proposed environmental taxes have driven industrial enterprises to improve their energy efficiency [5]. An exponential growth in research publications in the last two decades clearly shows the academic and practitioners' strong interests on this topic. The electricity demanded by CNC-enabled machine tools' servomotors on a factory shop floor produces energy consumption data that, when well-processed, is a valuable information source. Based on the data, energy consumption (EC) predictive models can be developed to enhance the sustainability of machining. Energy consumption models can be used to assess and improve the overall efficiency of shop floors, aid production engineers in scheduling optimisation, and support machining systems to be self-controlled and self-optimised through embedded optimal control algorithms. To develop effective EC models, research work must be carried out for both qualitative and quantitative understanding.

Recently, methods such as analysis of variance (ANOVA), Response Surface Methodology (RSM), Taguchi signal-to-noise ratio, and Artificial Neural Networsk (ANN) have been employed to analyse the relationships between cutting parameters and energy consumption, and establish energy predictive models [6]–[12]. Also, [13] carried out an experimental investigation on different machine tools using non-linear regression. The results show that the motion of the CNC machine tool is the primary source of energy consumption.

Many other researchers have used several approaches and techniques for understanding the energy consumption of CNC machining processes. A common way of energy and productivity assessment is through the Material Removal Rate (*MRR*) [8] and [9]. That is because the *MRR* is estimated based on key cutting parameters: spindle speed (S), feed rate (f), depth of cut (a_e) and width of cut (a_p). Although this approach simplifies the modelling process, since it comprises of two coefficients to be estimated and only one input is necessary, the *MRR*, by doing this, it assumes that all cutting parameters have the same effect on the energy consumption. Sealy *et al*. [14] observed low predictive accuracy of such models when employed estimating the net specific energy, or specific energy consumption for the state of engagement (SEC_{SoE}), which represents the amount of energy required to remove a unit volume of material during actual cutting (or engagement), that is, the energy required to maintain the CNC machine ON (known as basic and idling energy), and the energy consumed during air cutting (also known as travelling energy) are not considered. This way, this indicator is mainly influenced by the cutting parameters, workpiece material and tooling.

To date, there has been little research focused on the net specific energy [15]. Further, no effort has been made towards the implementation of machining net power and time estimation models to obtain optimum cutting parameters which can maximise the energy efficiency of milling operations. Other factors involved in the machining process, such as tool wear, mode of milling, types of cutter tool holder and workpiece holding systems, are still lacking analysis regarding their impact on energy consumption, so should be involved in the empirical modelling to develop more robust predictive models.

Based on that, this paper develops an effective energy consumption model considering the machining cutting variables spindle speed, feed rate and engagement depth (depth of cut and width of cut. Also, the machining net power (power load) is introduced for the first time to assess the cutting tool life.

2.2 Optimisation approaches for machining

The use of optimisation algorithms is a key step towards increasing machining efficiency, cost reduction and manufacturing sustainability. Significant efforts have been made by the research community to address complex manufacturing scenarios, involving environmental, legal, economic and quality requirements.

Table 1 shows related work and summarises the optimisation methods and objectives that have been used in recent years.

The energy consumption modelling and optimisation approach developed in this paper follows the required steps highlighted by [16] and [17], respectively, which are:

- Knowledge of the machining processes under analysis.
- Empirical equations of the objective(s) and constraint(s) to define the optimisation problem.

- Specifications for the CNC machine capabilities.
- Draw optimisation criteria and the problem formulation.
- Knowledge of mathematical and numerical optimisation techniques.

Table 1 Related work on the use of optimisation methods for machining processes

Related Work	Methods	Objectives	Cutting parameters
Wang *et al*. [18]	Pattern search (PS), Genetic algorithm (GA) and Simulated annealing (SA)	Energy consumption and Productivity	Cutting speed (v_c), a_p and a_e
Sonmez *et al*. [17]	Dynamic programming and Geometric programming	Production rate	v_c and feed per tooth (s_z)
Ozcelik *et al*. [19]	GA	Surface roughness	v_c, f, a_p and a_e
Sreeram *et al*. [20]	GA	Tool life	a_p
Li *et al*. [21]	GA	SEC and machining time	S, f, a_p and a_e
Baskar *et al*. [22]	GA, Hill climbing algorithm and Memetic algorithm	Maximum profit	S and f

As shown in Table 1, genetic algorithm is amongst the most popular algorithm for solving machining optimisation problems. Also, a considerable number of optimisation objectives have been considered. However, an efficient and reconfigurable optimisation strategy, especially considering both the specific energy and the manufacturing requirements for cutting tool life and productivity, has not yet been accomplished. The trade-offs involved between these criteria are the core motivations of this work.

3. EXPERIMENTAL DESIGN

3.1 Experimental set-up

The experimental trials were carried out on a 3-axis vertical milling machine Haas VF-3, which comprises a 30HP (22.4kW) 415 V vector drive, with maximum spindle speed of 8100 rpm.

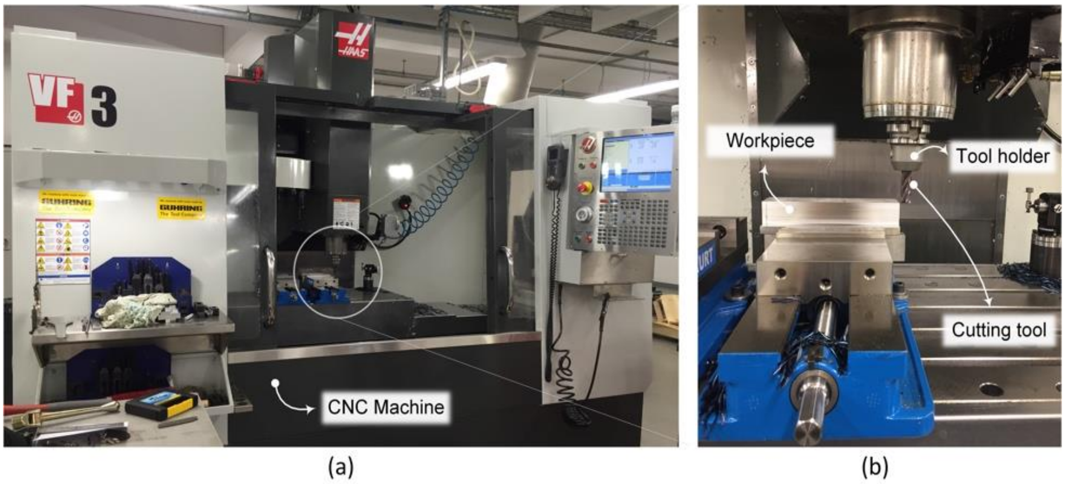

Fig. 1 (a) Haas VF-3 vertical milling machine (b) machined workpiece and cutting tool

BS EN24T alloy steel (AISI 4340) was selected as the workpiece material. There are two reasons for using this material: 1) the material is widely used for several engineering applications such as gear shafts, propellers, and so on [23]; 2) BS EN24T alloy steel is a hard material, and the energy consumption for machining hard materials is higher than that of mild and soft materials owing to the greater torque required during the cutting process. The material's properties are displayed in Table 2.

Table 2 The material properties for the workpiece

BS EN24T Alloy Steel (AISI 4340)		
Composition: C 0.36-0.44 / Si 0.10-0.35 / Mn 0.45-0.70 / S<0.040 / P<0.035 / Cr 1.00-1.40 / Mo 0.20-0.35 / Ni 1.30-1.70		
Property	Value	Unit
Density	7850	kg/m^3
Young's modulus	210	GPa
Hardness - Brinell	248-302	HB

The cutter tool used is a solid carbide (Table 3), held by a side-lock tool holder. The machining processes were carried out under dry conditions and up milling mode.

Table 3 Cutting tool specifications

Tool property	Specifications
Tool ID	End mills RF 100 DIVER No. 6736
Tool diameter (*D*)	16 mm
No. of teeth	4
Feed per tooth (s_z)	0.025 – 0.1 mm/tooth
Cutting speed (v_c)	150 – 250 mm/min
Corner radius	0.16 mm
Cutter material	Solid carbide.

The part selected is a jaw-type geometry with slotting features on both sides (Fig. 2). The tool-path strategy is a unidirectional route with constant tool engagement (linear motion). A safe clearance distance of 8 mm is set in the X direction for the cutting tool on the start and end of the machining process, and 1 mm clearance in Z. That is, the cutting tool travels 8 mm with the supplied feed rate before and after engaging onto the workpiece.

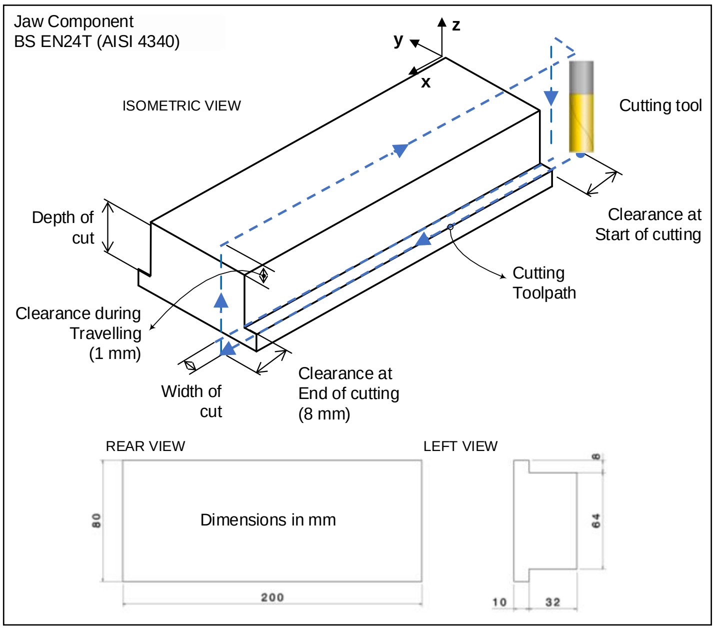

Fig. 2 CAD design of the machined metal component and dimensions

The power consumption is monitored by a Cyber Physical System (CPS) mounted on CNC machines with measuring frequency of 10 Hz (further specifications provided in Lu *et al.* [24]). Experiments were designed to analyse the significance and the interaction effects of spindle speed (*S*), feed rate (*f*) and width of cut (a_e) on the energy consumption for the roughing stage of milling. Firstly, five levels of cutting speed (v_c) and feed per tooth (s_z) were selected to calculate the experimental values for S and f. The selected levels range from the lower (Lo) and higher (Hi) boundaries of v_c and s_z, defined based on the machinist experience; and the recommended (Re) value by the tooling handbook is also included. This provides a good range for each parameter, which supports reliable observation of the relationship between inputs (*i.e.*, machining parameters) and the outputs (*i.e.*, power, energy and time).

The intermediate values: middle-low (M-L) and middle-high (M-H) of cutting speed (v_c) and feed per tooth (s_z) were obtained using the following Equations (1) to (4):

$$I_{v_c} = \left(v_{c_{Hi}} - v_{c_{Lo}}\right) / \left(n_{level} - 1\right) \tag{1}$$

$$v_{c_i} = v_{c_{i-1}} + I_{v_c} \tag{2}$$

$$I_{s_z} = \left(s_{z_{Hi}} - s_{z_{Lo}}\right) / \left(n_{level} - 1\right) \tag{3}$$

$$s_{z_i} = s_{z_{i-1}} + I_{s_z} \tag{4}$$

where I is the interval between each level of v_c, and s_z; i stands for the intermediate levels M-L and M-H; n_{level} is the number of levels desired, which 5 levels are chosen in this study (this impacts on the number of experimental trials and resources available).

The levels of spindle speed (S), feed rate (f) and width of cut (a_e) are obtained based on the levels of v_c, and s_z, and the tool diameter (D), using the following Equations (5) to (7).

$$S_i = v_{c_i} \cdot 1000 / \pi \cdot D \tag{5}$$

$$f_i = N \cdot s_{z_i} \cdot S_i \tag{6}$$

$$a_{e_i} = a_{e_f} / n_{pass_i} \tag{7}$$

where D is the diameter of the cutter; N is the number of tool teeth; i stands for the different levels (Lo, M-L, M-H and Hi); a_{e_f} is the final width from the part design; n_{pass_i} is the *i-th* number of cutting passes based on the a_e value, and it must be an integer. The maximum a_e supported by the process is 4 mm, which has been revealed by pre-experimental testing considering the actual machining holding and fixtures capabilities.

Table 4 shows the levels of the cutting parameters obtained according to the above Equations.

Table 4 Cutting parameters

Levels	v_c / mm min^{-1}	D / mm	N / tooth	s_z / mm tooth^{-1}	S / rpm	f / mm min^{-1}	a_e / mm
1. Re	200.0	16	4	0.070	4000	1115	4.00
2. Lo	150.0	16	4	0.025	3000	300	1.60
3. M-L	184.5	16	4	0.059	3670	870	2.00
4. M-H	218.7	16	4	0.082	4350	1430	2.67
5. Hi	250.0	16	4	0.100	5000	2000	4.00

3.2 Design of experiments

Taguchi fractional factorial was used to define the design of experiments, and a total of 24 experiments were carried out based on the orthogonal principle. Moreover, Material Removal Rate (*MRR*) is a significant evaluation factor on the energy consumption [15]. Thus, to evaluate the results considering this factor, the *MRR* of each trial is calculated using Equation (8).

$$MRR = f \cdot a_e \cdot a_p = \left(v_c \cdot 1000 \cdot N \cdot s_z / \pi \cdot D\right) \cdot a_e \cdot a_p \tag{8}$$

where a_p is the depth of the cut (in this research, it was chosen 32 mm as the full depth of the designed part); and *MRR* is the material removal rate in mm^3/min.

To correlate the *MRR* as an indicator for the productivity and facilitate decision-making, the minimum and maximum calculated values of *MRR* have been used to define the lowest (Lo) and Highest (Hi) productivity levels. While the intermediate levels were defined heuristically considering the distribution of *MRR* values within the range. Table 6 shows the experimental design, including the machining parameters and productivity levels.

Table 5 Experimental design based on orthogonal principle

Trial	S / rpm	f / mm min^{-1}	a_e / mm	a_p / mm	MRR / mm^3 min^{-1}	Productivity Level
1	3000	1115	4.00	32	142720	M
2	3670	1115	4.00	32	142720	M
3	4350	1115	4.00	32	142720	M
4	5000	1115	4.00	32	142720	M
5	4000	300	4.00	32	38400	Lo
6	4000	870	4.00	32	111360	M-L
7	4000	1430	4.00	32	183040	M-H
8	4000	2000	4.00	32	256000	Hi
9	3000	870	4.00	32	111360	M-L
10	3000	1430	4.00	32	183040	M-H
11	3000	2000	4.00	32	256000	Hi
12	3670	870	4.00	32	111360	M-L
13	3670	1430	4.00	32	183040	M-H
14	3670	2000	4.00	32	256000	Hi
15	4350	870	4.00	32	111360	M-L
16	4350	1430	4.00	32	183040	M-H
17	4350	2000	4.00	32	256000	Hi
18	5000	870	4.00	32	111360	M-L
19	5000	1430	4.00	32	183040	M-H
20	5000	2000	4.00	32	256000	Hi
21	4000	1115	1.60	32	57088	M-Lo
22	4000	1115	2.00	32	71360	M-L
23	4000	1115	2.67	32	95266	M-L
24	4000	1115	4.00	32	142720	M

3.3 Experiment results

During the 24 experimental trials, the power data monitored as a function of time shows that different sets of machining parameters generated different power profiles. Fig. 3 shows the power profiles of trials, which demonstrate the impacts of parameter sets on machining time and power loads.

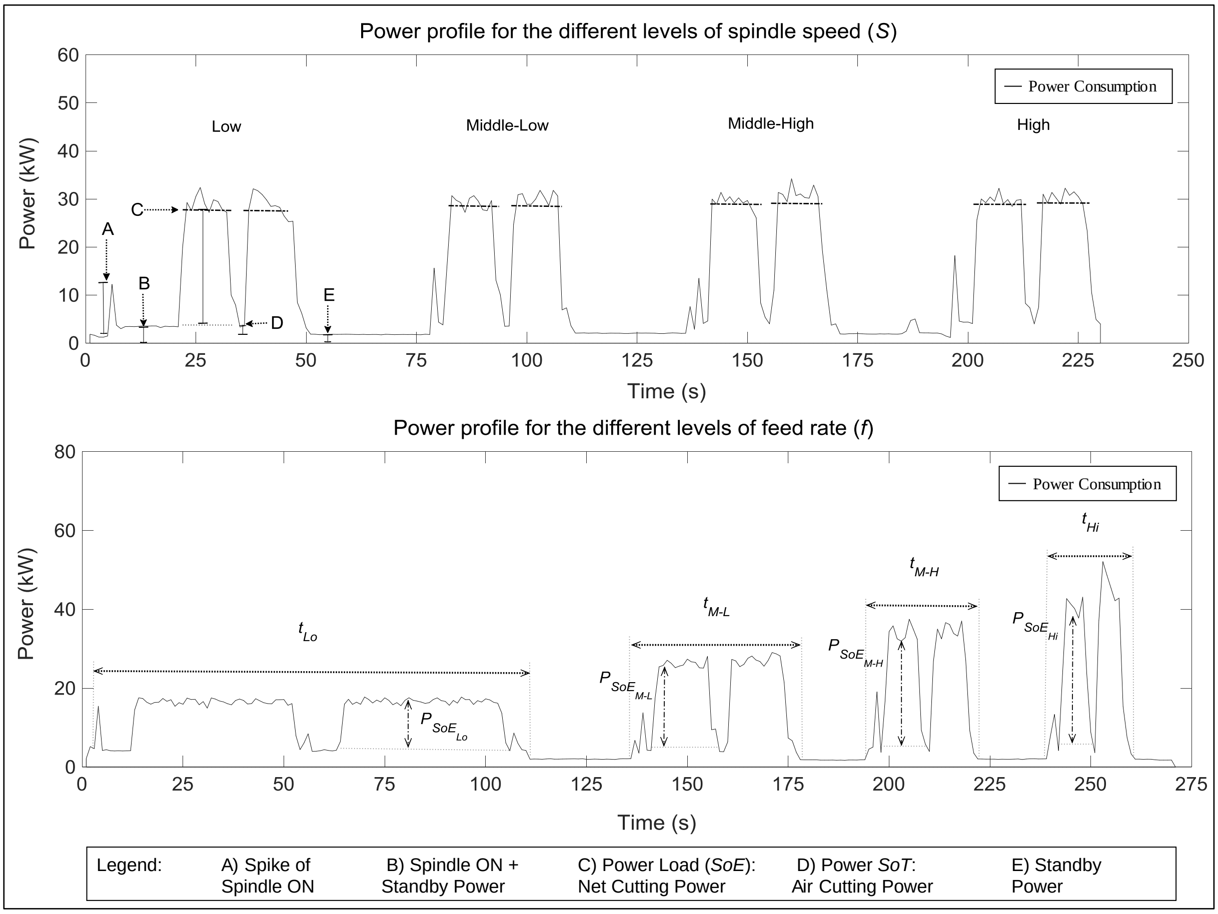

Fig. 3 Power profile of machining experiments on BS EN24T Alloy workpiece (a) *Spindle speed* analysis: power load in C is not significantly affected from Lo to Hi levels of *S* (b) *Feed rate* analysis: power load (P_{SoE}) increases, while machining time (*t*) decreases significantly from Lo to Hi levels of *f*

The data obtained from the CPS and sensors (Lu *et al*. [24]) was analysed considering two distinct machining states: state of engagement (SoE) and state of non-engagement travelling (SoT). The former represents the process of material removal (actual cutting), while the latter represents non-cutting movements (air cutting). $\bar{P}_{SoE}$, which is the average of the power of SoE (*i.e.*, P_{SoE}), is introduced to assess the electricity consumption performance during a machining process. Similarly, $\bar{P}_{SoT}$ is the average of the power of SoT (*i.e.*, P_{SoT}). Energy consumption EC_{SoE} and EC_{SoT} are the total energy consumption for SoE and SoT respectively. Specific Energy Consumption (*SEC*) during the SoE is used to indicate the machine energy efficiency when removing materials [25]. The relevant computations are in the following Equations (9) to (13).

$$\bar{P}_{SoE} = \int_{t_1}^{t_{SoE}} P_{SoE} dt \,/ \sum_{n_{pass_1}}^{n_{pass_n}} t_{SoE} \tag{9}$$

$$\bar{P}_{SoT} = \int_{t_1}^{t_{SoT}} P_{SoT} dt \,/\, t_{SoT} \tag{10}$$

$$EC_{SoE} = \int_{t_1}^{t_{SoE}} P_{SoE} dt \tag{11}$$

$$EC_{SoT} = \int_{t_1}^{t_{SoT}} P_{SoT} dt \quad (12)$$

$$SEC_{SoE} = EC_{SoE} / V \quad (13)$$

where V is the volume removed during machining, t_{SoE} is the machining time during SoE for each cutting pass n.

The data collected using the smart sensor network for power consumption and time of all experimental trials were treated using data analysis software and are summarised in Table 6. The sensor system was calibrated by commercial company before running the experimental trials.

Table 6 Experimental results for milling on BS EN24T alloy steel

Trial	EC / kJ		% SoT	t / s		$\bar{P}_{SoE}$ / kW	Cutting Tool Life Level	SEC_{SoE} / kJ cm^{-3}	Energy Efficiency Level
	SoE	SoT		SoE	SoT				
1	580	92	14	20	10	29	M	11	M-H
2	595	94	14	20	10	30	M	12	M-H
3	608	97	14	20	10	30	M	12	M-H
4	603	100	14	20	10	30	M	12	M-H
5	1297	128	9	78	21	17	Hi	25	Lo
6	694	94	12	26	11	27	M-H	14	M-H
7	544	79	13	16	8	34	M-Lo	11	M-H
8	497	63	11	12	6	41	M-Lo	10	Hi
9	1519	185	21	80	23	19	Hi	20	M-L
10	1222	146	19	63	17	21	M-H	16	M
11	1199	103	8	48	13	25	M-H	16	M
12	1011	61	6	32	9	32	M-L	13	M-H
13	1066	86	7	40	10	27	M-H	14	M-H
14	878	88	9	24	8	37	M-Lo	11	M-H
15	650	143	18	16	9	41	Lo	8	Hi
16	1105	97	8	40	10	28	M-H	14	M
17	828	107	11	24	8	35	M-L	11	M-H
18	675	142	17	16	9	42	Lo	9	Hi
19	1118	97	8	40	10	28	M-H	15	M
20	848	106	11	24	8	35	M-L	11	M-H
21	686	146	18	16	9	43	Lo	9	Hi
22	1158	107	8	40	10	29	M	15	M-H
23	902	113	11	24	8	38	Lo	12	M-H
24	688	159	19	16	9	43	Lo	9	Hi

4. QUALITATIVE ANALYSIS ON EXPERIMENTS

Qualitative analysis is an efficient means for obtaining knowledge from a complex environment, and thus this method is used in this section to understand the relationships of key cutting parameters in machining processes and the energy consumption to produce BS EN24T (AISI 4340) parts.

The analysis of the significance of the key parameters on the energy consumption reveals the important order of relationships between each input and this response and supports the selection of the correct mathematical model for the optimisation.

The results of $\bar{P}_{SoE}$ and SEC in Table 6 show that the machining performance (analysed through the power, energy and time) is highly affected by the selection of machining parameters and key trade-offs have been identified. For instance, Trial 24 requires the highest power load, 43 kW, while Trial 5 presents the lowest, 16.53 kW. Nevertheless, the energy efficiency of Trial 24 (SEC=9 kJ/cm^3) is lower than that of Trial 5 (SEC=25 kJ/cm^3), that is due to the greater machining time spent for Trial 5.

In addition, there are two main observations based on the results for the energy consumed during the SoE and SoT:

- The energy required for air travelling (SoT) is between 6% to 21% of the overall EC (EC_{SoE}+EC_{SoT}) for all trials. The results reveal that the amount of energy consumed during the SoE is the most representative over the SoT. Moreover, SoE is varied from 79% to 94% of the overall energy consumed. Consequently, the investigation finds that the machining parameters play an even more critical role on the energy efficiency of the production.
- Based on the energy results for SoT, it is observed that the amount of energy varies significantly between the experimental trials. This was caused by the different safe clearance distance set in the NC code, in which the cutting tool moves with the supplied feed rate and spindle speed (*i.e.*, the experimental values) to approach the workpiece. These observations are machine-dependent (e.g., vector drive horsepower and drive technology).

The effects of machining parameters, spindle speed (S), feed rate (f) and width of cut (a_e) on the power, energy and time required during SoE are investigated as follows.

4.1 Spindle Speed effects

The main effects of spindle speed on the power load and energy are analysed. The results of the experiments are presented in Fig. 4.

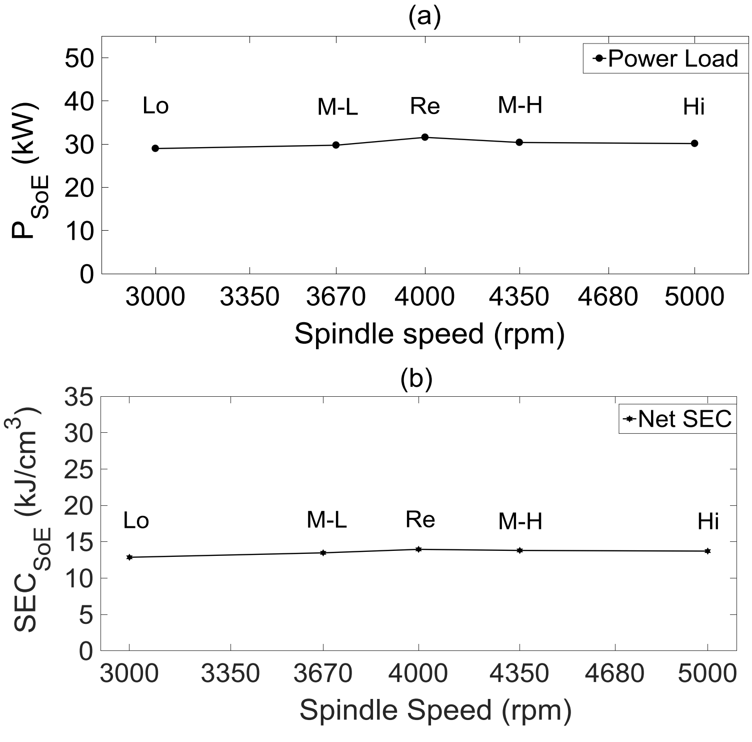

Fig. 4 Experimental results on BS EN24T alloy (a) Relationship between S and $\boldsymbol{\overline{P}_{SoE}}$, mean power oscillation is ± 5% (b) Relationship between S and SEC

The main results from the experimental trials show that:

- Changes in S do not generate substantial effects on $\overline{P}_{SoE}$, as shown in Fig.4(b). S does not affect the machining time as prior known.
- During the travelling time, more energy is wasted at higher levels of spindle speed, since the spindle motor requires more power at higher speeds. An increasing energy demand of approximately 3% between each level of S is revealed.

- The power load $\bar{P}_{SoE}$ increases slightly from the Lo until the Re levels of S. Beyond this level, a slight drop of $\bar{P}_{SoE}$ is identified (shown in Fig. 4(a)). This way, the M-H level is the point at which increasing S, when all other parameters are kept constant, the amount of material removed per cutting tool revolution has a positive effect on the energy consumption. Consequently, the cutting load per unit time is smaller. High levels of S promote a slight decrease in the power load ($\bar{P}_{SoE}$).
- S does not have substantial effects on the energy efficiency, as shown in Fig.4(b).

The results show that a selection of Lo or Hi levels of S is more appropriate to achieve energy efficiency in machining processes (Fig. 4(b)), although higher machining speeds are known to decrease the cutting tool life [26].

4.2 Feed Rate effects

Feed rate (f) is one of the major factors that determines the material removal rate (*MRR),* as shown in Equation (8). That is, the increase in f and maintaining other parameters unchanged will lead to a greater *MRR*. Fig. 5 shows the results for the experimental trials for the feed rate analysis.

The main findings of this experimental investigation are:

- Substantial effects of the feed rate f on the power load $\bar{P}_{SoE}$ and machining time t_{SoE} are observed. Through the standard deviations of the power load ($\sigma_{f_{P_{SoE}}} = 8$, and mean $\bar{x}_{f_{P_{SoE}}} = 30$ kW), and machining time ($\sigma_{f_t} = 26$, and mean $\bar{x}_{f_t} = 33$ s), these values show that f generates a greater impact on the machining time compared to the power load, in approximately 3 times. It could be conflicting when considering a sustainable process, since the increase in the feed rate would increase the productivity rate but, at the same time, increase the power load.
- Increasing the feed rate reduces the machining time, as shown in Fig. 5(a). The machining time is reduced by approximately 85% at the maximum level of f when compared to the lowest level of f.
- Increasing the feed rate increases the machining power load, as shown in Fig. 5(b). The power load f at the Hi level is approximately 3 times greater than at the Lo level of f.
- A High feed rate promotes better energy efficiency owing to savings in machining time. The process at the Lo level required 2.6 times more specific energy (kJ/cm^3) compared to the Hi level, shown in Fig. 5(c). However, the drawback is that it produces higher cutting forces and higher temperatures at the cutting tool, consequently, shortening the tool life.

The results suggest that the selection of M-L or M-H cutting feed levels are more appropriate to make a balance between energy, time and cutting tool life.

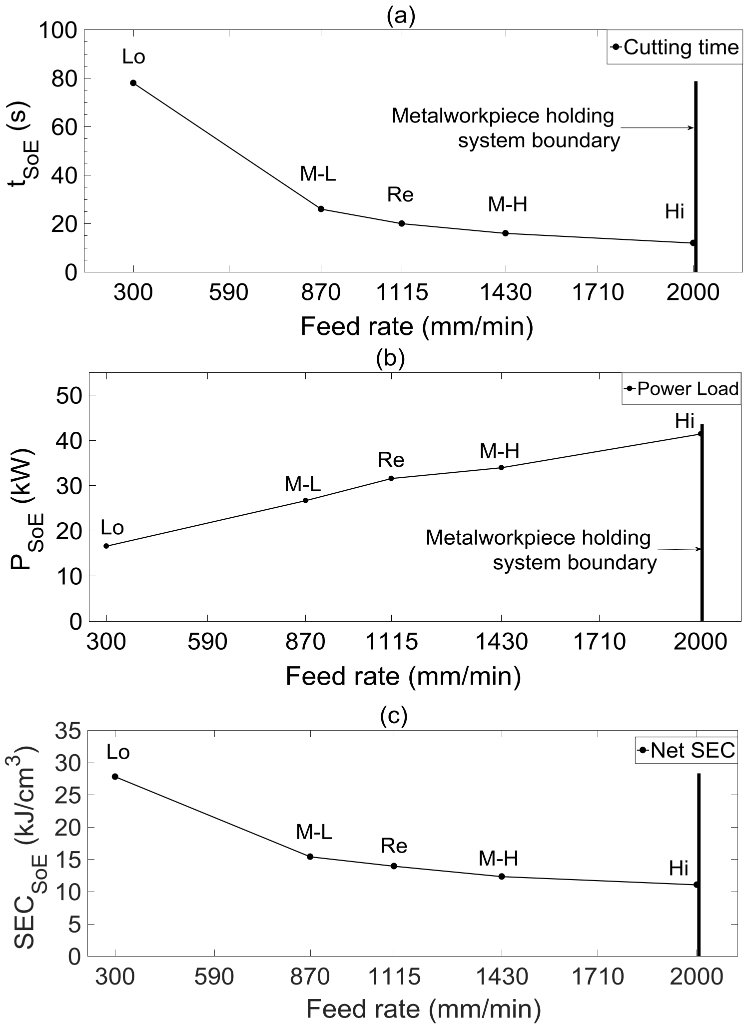

Fig. 5 Experimental results on BS EN24T alloy (a) Relationship between t_{SoE} and f (b) Relationship between f and $\bar{P}_{SoE}$, mean power oscillation is ± 5% (c) Relationship between SEC *and* f

4.3 Width of Cut effects

Width of cut influences MRR in a machining process, as shown in Equation (8). The experimental results of a_e on machining processes are presented in Fig. 6.

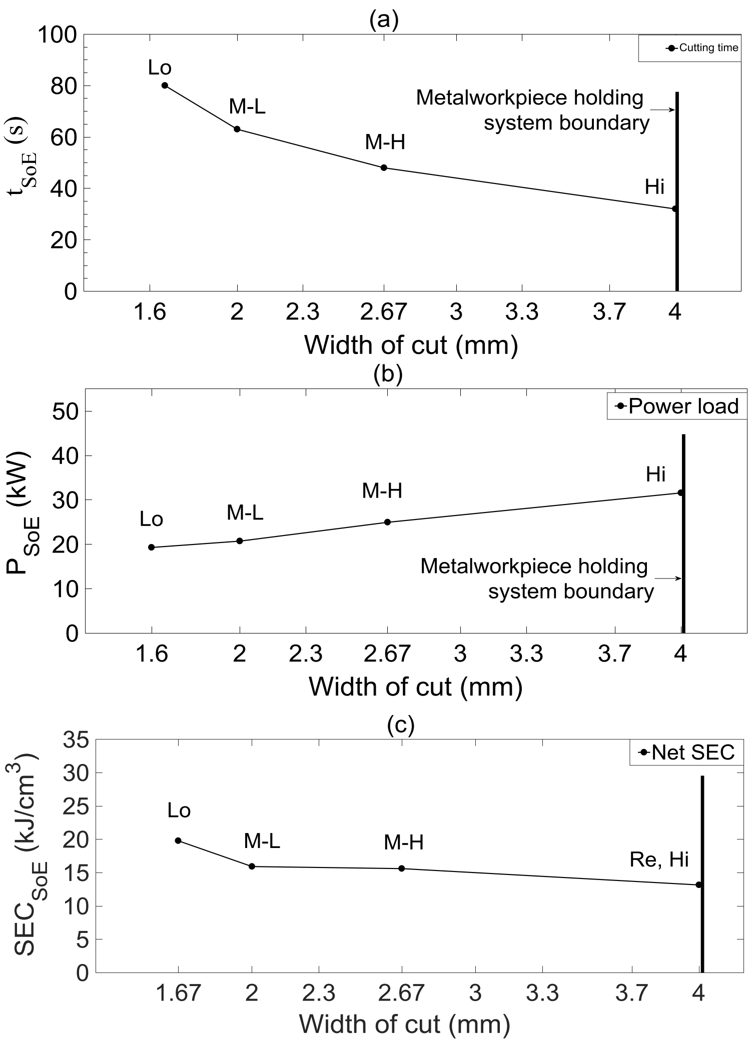

Fig. 6 Experimental results on BS EN24T alloy (a) Relationship between t_{SoE} and a_e (b) Relationship between a_e and P_{SoE}, mean power oscillation is ± 5% (c) Relationship between SEC and a_e

Significant effects of a_e on the power load, machining time and energy efficiency are revealed. A summary of the observations is provided below:

- The clarify the significant effects of a_e on the power load and machining time, the standard deviations and means are provided as follows. For the power load $\sigma_{a_{eP_{SoE}}} = 7$, and mean $\bar{x}_{a_{e\,P_{SoE}}} = 24$ kW. For the machining time, $\sigma_{a_{e_t}} = 24$, and mean $\bar{x}_{a_{e_t}} = 56$ s. These values show that changes in the width of cut will affect the machining time 3.5 times more than the power load, which supports positively a trade-off when considering productivity and cutting tool life.
- Increasing the width of cut gives significant decrease in machining time, as shown in Fig. 6(a). The machining time at the Hi level was 60% shorter compared to time at the Lo level.
- Increasing the width of cut increases the radial contact between the cutter tool and the workpiece. It causes higher stress and power load for material removal. Consequently, it increases the workload at the tool, which can be seen through the power load response shown in Fig. 6(b). The results reveal that the power load at Hi level (4 mm) is 38% greater than at the Lo level (1.67 mm), and furthermore, it is described by a nonlinear relationship.
- A High width of cut will give a more energy-efficient process owing to reductions in machining time. However, the drawback is the higher power load, which means greater cutting forces and chip load on the cutter tool, consequently, shortening the tool life. For instance, at Hi level of a_e the operation was 33% more energy efficient compared to the Lo level shown in Fig. 6(c).

The results suggest that the selection of M-L or M-H levels are more appropriate when considering energy, time and tool life for a sustainable process.

Nevertheless, the trade-offs revealed by the qualitative analysis emphasise that the selection criteria of optimal cutting parameters should also consider production constraints such as lead time or cutting tool availability; otherwise the process is not productive, energy efficient nor improves the cutting tool life. This observation is considered further in the optimisation problem.

5. OPTIMISATION ON ENERGY CONSUMPTION

In this section, an optimisation problem is presented considering the experimental results presented in Section 4. In addition, the fitness functions for the optimisation, *i.e.*, energy efficiency, cutting tool life and productivity are defined.

5.1 Optimisation modelling

The energy required during the state of engagement (SoE) for the milling on BS EN24T alloy (AISI 4340) accounted for 79% to 94% of the overall energy consumption. Therefore, significant energy saving in machining processes is possible if the energy during SoE, (EC_{SoE}) could be minimised. The following formulas represent EC_{SoE} and the related parameters:

$$t_{SoE} = V/MRR \tag{14}$$

$$EC_{SoE} = \bar{P}_{SoE} \cdot t_{SoE} = \bar{P}_{SoE} \cdot V/MRR \tag{15}$$

$$\bar{P}_{SoE} = f_1\left(S, f, a_e \cdot a_p\right) \tag{16}$$

$$MRR = f_2\left(f, a_e, a_p\right) = f \cdot a_e \cdot a_p \tag{17}$$

where $\bar{P}_{SoE}$ is the average power used during SoE, V is the removed volume of material, MRR is the material removal ate, S, f, a_e, a_p are the cutting parameters spindle speed, feed rate, width of cut and depth of cut, respectively.

In order to establish the function of $\bar{P}_{SoE}$, a Responsive Surface Regression Model was developed. The model structure is presented below:

$$P_{SoE} = \beta_0 + \beta_1 \cdot S + \beta_2 \cdot f + \beta_3 \cdot a_e a_p + \beta_{11} \cdot S^2 + \beta_{22} \cdot f^2 + \beta_{12} S \cdot f \tag{18}$$

where $\beta_{0,1,2,11,12,22}$ are coefficients to be determined.

Apart from experimental trials 4, 5, 9, 10, 14 and 23 (which are later used for model validation) other trials were used to generate the coefficients. The output data was filtered using a single exponential smoothing technique. This is an additional step prior to the coefficient estimation process to reduce the random fluctuations in the time series for the collected data, thus, providing a more accurate pattern of the power load of each experimental trial. By taking this step, the accuracy of the final predictive model is increased by 2.92%. Subsequently, non-linear regression and least squares methods are employed to estimate the model's coefficients. The estimated coefficients $\beta_{0,1,2,11,12,22}$ are given in Table 7. The accuracy of the smoothed model is R^2-adjusted equal to 0.94, which shows the achievement of satisfactory predictive accuracy.

Table 7 Power load model coefficients

Coefficient	Value	Significance (P value: α < 0.05) *
β_0	–16.1700	0.000
β_1	0.00577	0.036
β_2	0.01225	0.000
β_3	0.1751	0.000

β_{11}	–0.0000010	0.001
β_{22}	–0.0000020	0.000
β_{12}	0.0000020	0.005

** Interval of confidence is 95%, i.e., α=0.05.*

This model was validated using data collected from experimental trials 4, 5, 9, 10, 14 to 23. The results of the estimated $\bar{P}_{SoE}$ presents a predictive accuracy R^2 of 0.98, which shows good performance.

From Equation (15), it can be observed that to minimise EC_{SoE}, $\bar{P}_{SoE}$ should be minimised and *MRR* should be increased. Based on this, an optimisation objective (fitness) to minimise SEC_{SoE}, the indicator for the energy efficiency, is set up below:

$$\begin{cases} Minimise\ SEC_{SoE} = \rho_1 \cdot \bar{P}_{SoE} + \rho_2 \cdot 1/MRR \\ Subject\ to: \\ \qquad 150 \le x_1 \le 250 \\ \quad 0.025 \le x_2 \le 0.10 \\ \quad 51.20 \le x_3 \le 128 \end{cases} \tag{19}$$

where x_1, x_2 and x_3, are cutting speed, feed per tooth and engagement depth, respectively; and, ρ_1 and ρ_2 are weights, where $\rho_1 + \rho_2 = 1$.

$\bar{P}_{SoE}$ is also related to the cutting tool's life. Increases of $\bar{P}_{SoE}$ will generate increases in cutting forces and temperature on the cutting tool so that the life of the tool will be reduced. *MRR* represents the process productivity. Regarding the setting of the two weights, a strategy has been designed heuristically based on the relevance of the power load and material removal rate to the cutting tool life and productivity, respectively, as well as personal communications with experts in the field. The strategy for the settings can be defined as presented in Table 8.

Table 8 Production weighting strategy

Description	Weighting Selection*
Cutting tools are the major constraint.	$0.8 \le \rho_1 \le 0.9$
Cutting tools are more constrained than lead time.	$0.5 < \rho_1 < 0.8$
Both resources are constrained.	$\rho_1 = \rho_2 = 0.5$
Lead time is more constrained than cutting tools.	$0.5 < \rho_2 < 0.8$
Lead time is the major constraint.	$0.8 \le \rho_2 \le 0.9$

**Weights law:* $\rho_1 + \rho_2 = 1$

The appropriate strategy is chosen by the engineer or process planer based on the immediate availability of the resources, cutting tools, and lead time – or which has the greatest priority – in the factory. After that, the appropriate weights, ρ_1 and ρ_2, are selected from the weighting strategy table and combined with the objective function for energy saving. Consequently, the importance of the objective within the optimisation process is reconfigured to align these with the factory's immediate requirements. As a result, the optimal solution achieved by the optimisation process for the machining operation is also the best solution for the factory.

5.2 Optimisation algorithm: improved multi-swarm fruit-fly optimisation algorithm (iMFOA)

An improved optimisation algorithm, based on the recent fruit fly optimisation algorithm (FFOA), was initially considered to solve the optimisation problem formulated in Section 5.1. FFOA is a nature-inspired algorithm for solving optimisation problems by mimicking the highly-advanced sense of smell of insects to detect food locations [27]. This modern algorithm has presented outstanding performance on solving optimisation problems, especially in business and finance areas which require highly reliable predictions [28]–[31]. However, its ability to solve trade-offs of machining parameters has not yet been fully investigated.

To address this gap, a multi-swarm fruit fly optimisation algorithm (MFOA) developed by [32] was then improved to cope with the machining optimisation. The problem formulated in Section 5.1

comprises three input variables (*i.e.*, machining parameters) which are constrained by the safe boundaries. However, the MFOA algorithm is designed to solve problems with two non-constrained input variables. Thus, further improvements were made to the original MFOA algorithm. Major changes to achieve the improved MFOA (iMFOA) can be found below:

- A third axis is included to specify the fruit fly coordinates (*i.e.*, positions), so the algorithm can cope with the three input variables.
- A sphere function is embedded to define the search space, *i.e.*, the fruit flies' flying space, so ensuring the cutting parameters selected are within the safe boundaries.
- A penalty function is included to constrain the power load fitness function, which cannot be above a certain level to guarantee energy sustainability.

Fig. 7 shows the algorithm schematic and illustration of the iMFOA.

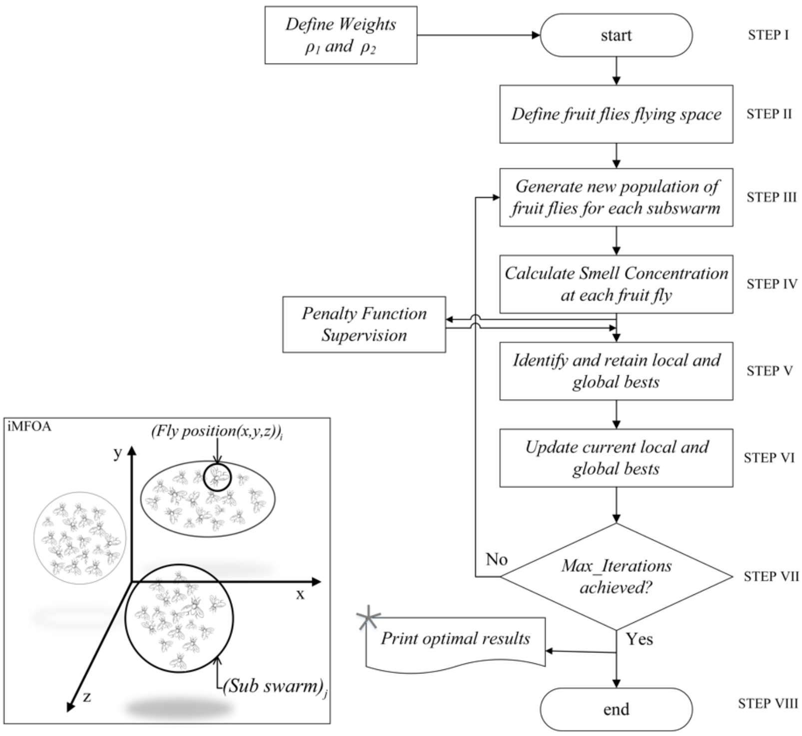

Fig. 7 Flowchart of the improved MFOA (iMFOA) algorithm

Firstly, an engineer or process planner defines the production weights (i.e., ρ_1 and ρ_2), to align the optimisation engine with the production constraints so the algorithm can be initialised (STEP I). Then, based on the process safe boundaries (calculated in STEP II) the fruit flies' populations (*i.e.*, sub swarms) are generated in STEP III. Each fruit fly position, *i.e.*, $(x, y, z)_i$, represents a combination of the cutting parameters S, f and $a_p \cdot a_e$. This process can be represented as follows:

$$X_{new}(i,j) = x_{initial}(i,j) + randi(boundaries_{SpindleSpeed}) \tag{21}$$

$$Y_{new}(i,j) = y_{initial}(i,j) + randi(boundaries_{FeedRate}) \tag{22}$$

$$Z_{new}(i,j) = z_{initial}(i,j) + randi(boundaries_{EngagementDepth}) \tag{23}$$

where X, Y and Z_{new} are the fruit flies' positions of the new populations; i is the fruit fly and j is the sub swarm; x, y and $z_{initial}$ are the initial positions which are set to be zero at the start; *randi* is a computational function to select the respective values within the cutting parameters minimum and maximum boundaries;

To calculate the smell concentration (fitness) of each fruit fly, in STEP IV, the new populations for fruit flies are called into each of the fitness function, *i.e.*, *SEC*, $\bar{P}_{SoE}$ and *MRR*. In the optimisation problem, these fitness functions are combined to save computational time as follows:

$$Smell_{SEC}(i,j) = \rho_1 \cdot \bar{P}_{SoE}(i,j) + \rho_2 \cdot 1/MRR(i,j) \tag{24}$$

The output values of $\bar{P}_{SoE}$ and smell concentration are evaluated by a penalty function which judges the energy efficiency and cutting tool life based on the knowledge embedded into the system. If the power load is above the thresholds defined empirically, it reduces the smell concentration considerably. This supervisory loop ensures that inefficient cutting conditions are not identified as local or global best, in STEP V and, consequently, not retained in STEP VI.

Fruit flies (*i*) with the highest smell concentration within a sub swarm (*j*) are identified as local bests, while the global best is represented by the fruit fly with highest smell concentration among all sub swarms. Further, the local bests are used to substitute the initial positions and generate the new populations in the next iteration. This process occurs recursively until the maximum number of iterations is reached, so the global best fruit fly, which holds the optimal cutting parameters, and smell concentration path are achieved.

5.3 Case Study for validation of optimisation approach

A case study including three real-case manufacturing scenarios are presented in this section. This way, the proposed optimisation problem and iMFOA algorithm can be assessed. This will be done by evaluating the optimisation outputs considering some key rules to achieve sustainable machining.

The details of the manufacturing scenarios are given in Table 9.

Table 9 Manufacturing scenarios for the optimisation problem

Real-case scenarios of factory immediate requirements	Production Constraints
a) The production batch requires highly expensive cutting tools; however, the lead time is also a constraint since the penalty for not meeting the deadline is high.	Both resources are constrained. $\rho_1=\rho_2 = 0.5$
b) The deadline for delivering the production order has been extended; the manager asks to reconfigure the machining operations to prolong cutting tool life.	Cutting tools become the constraint. $\rho_1=0.8$, $\rho_2=0.2$
c) The deadline for delivering the production order has been shortened; the manager asks to reconfigure the machining operations to boost the productivity.	Lead time becomes the constraint. $\rho_2=0.8$, $\rho_1=0.2$

Specific energy consumption (*SEC*), power load (P_{SoE}) and material removal rate (*MRR*) are used as Key Sustainable Indicators (KSI) for the energy efficiency, cutting tool life and productivity, respectively. Furthermore, the optimal performances are analysed considering the rules for sustainable machining, as below:

- The smaller the *SEC* the better the energy efficiency.
- The greater the *MRR* the better the productivity.
- The smaller the P_{SoE} the better the cutting tool life.

Accordingly, the optimisation results for each manufacturing scenario will be discussed based on the above rules. This further supports the selection of the best result amongst the three optimisation algorithms employed for benchmarking analysis: GA [33], FFOA [27] and the iMFOA, presented in Section 5.2.

The details for the algorithm initialisation are: the production constraints' weights are defined heuristically based on each scenario characteristics. Then, the initial set up for the algorithm engine is defined as: number of sub swarms equal to 10, size of population of fruit flies per sub swarm equal to 25, and maximum number of iterations equal to 1000.

The optimisation algorithm was run under the initial set-up. Fig. 8 shows the smell concentration path containing the global best values during the convergence to the optimal solution from the iMFOA algorithm. Based on this figure, the algorithm does not present significant improvements in the smell concentration beyond 375 iterations. As the computation time is a critical factor to indicate the system performance of an online optimisation, 400 iterations are selected in this work as a trade-off between computation time and system performance.

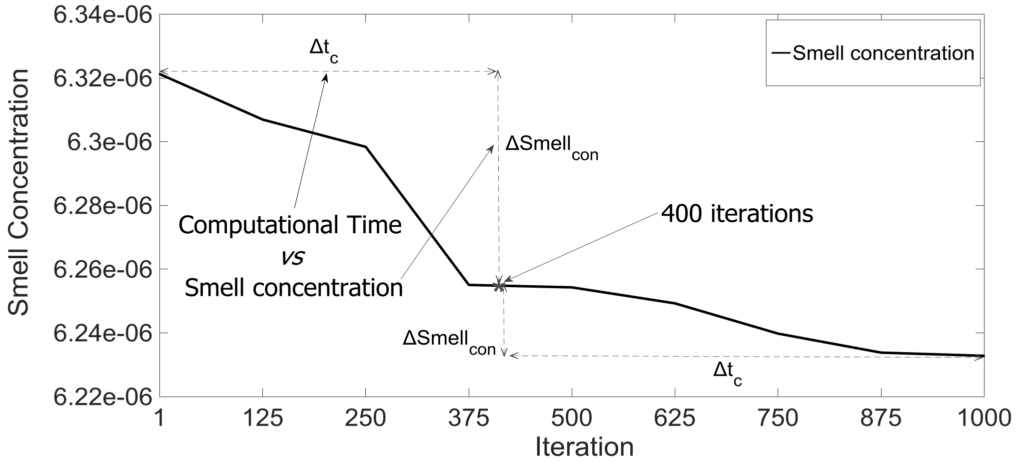

Fig. 8 Smell concentration path during optimisation using the iMFOA algorithm

Table 11 shows the optimisation results, *i.e*., optimal cutting parameters and estimated *SEC*, *MRR* and P_{SoE}, obtained from the algorithms used to solve the three manufacturing scenarios.

Table 11 Optimisation results and KSI

Scenario Constraint		*Optimisation Algorithm*	*Optimal Cutting Parameters*			*Key Sustainable Indicators*		
			Cutting Speed / mm min^{-1}	**Feed per tooth / mm tooth^{-1}**	**Engagement depth / mm**	**SEC / kJ cm^{-3}**	**MRR / cm^3 min^{-1}**	**Power Load / kW**
a)	Lead time and Cutting tools	iMFOA	**250.3**	**0.0336**	**80.10**	**17.6***	53.7	15.8
		FFOA	167.8	0.0444	103.30	**20.1**	61.3	20.6
		GA	250.4	0.0338	77.59	**17.7**	52.2	15.4
b)	Cutting tools	iMFOA	**151.1**	**0.0188**	**55.00**	15.8	20.6	**5.4***
		FFOA	175.2	0.0259	58.80	24.8	21.2	**8.8**
		GA	237.8	0.0212	52.00	17.9	20.9	**6.3**
c)	Lead time	iMFOA	**250.2**	**0.1236**	**105.70**	12.7	**157.2***	33.4
		FFOA	152.5	0.0611	90.60	18.3	**67.1**	20.5
		GA	163.4	0.1096	107.12	13.1	**152.8**	33.5

**Optimal value based on rules and manufacturing requirements.*

The results from the optimisation process highlighted in Table 11, are summarised below:

- From case *a)*, since both technical requirements lead time and cutting tools are constrained, the best solution will be decided considering the most energy-efficient process. That is, the set of machining parameters that provides the lowest specific energy consumption represents the optimal solution for this scenario. From Table 11, the results of the iMFOA algorithm promote the most energy efficient process, indicating this is the optimal solution. Although the genetic algorithm shows similar performance, when compared to traditional fruit fly algorithm, the iMFOA results promote better energy savings, approximately 12% more energy efficient.
- From case *b)*, cutting tools are the production constraint, and as stated previously, the lifetime of the cutting tools is proportionally correlated with the power load. Consequently, the best solution will

be decided considering the lowest power load value. From Table 11, the iMFOA is able to predict conditions that have 13% lower power load in comparison with the popular GA algorithm, or 38% improvement compared to the FFOA algorithm.

- From case *c)*, lead time is the production constraint. The best solution will be decided considering the highest material removal rate value. From Table 11, *MRR* obtained from the results obtained by iMFOA presents 3% better performance compared to GA, and 134% improvement when compared to traditional fruit fly algorithm.

Thus, the results from the iMFOA algorithm showed better performance, especially when compared to the FFOA algorithm. This validates the improvements made to the previous MFOA and the advantages of using this swarm algorithm in machining optimisation.

This case study uses real-case manufacturing requirements to validate the optimisation approach proposed in this research. Furthermore, it proves that the weighting strategy is an easy and effective method to align the manufacturing requirements, this way, bridging the gaps between ideal academic solutions and best practical solutions for the industry sector.

6. CONCLUSIONS

To achieve energy-efficient CNC machining processes, it is essential to develop effective analysis and optimisation approaches to evaluate the impact of machining parameters on energy consumption, and identify optimal parameters. In this paper, via experiments and qualitative analysis, key machining parameters affecting energy efficiency have been analysed in detail. The findings facilitate machining process planners in choosing suitable machining parameters to minimise energy consumption during machining. Based on the analysis, an improved multi-swarm fruit fly optimisation algorithm has been developed to optimise machining parameters. Case studies and benchmarking have been conducted to test the algorithm. The main conclusions are:

1) The feed per tooth has the most significant effect on the machining time, specific energy and power load. For energy-efficient CNC machining, high feed rates are suggested due to the savings in machining time; however, if cutting tools limit production, the optimal machining conditions should be reconfigured to low levels of feed per tooth and cutting speed, while the engagement depth should be recommended by the tooling handbook.
2) The developed optimisation approach is an effective tool to fine-tune the key machining parameters to guarantee energy efficiency during machining processes, and furthermore meet the requirements for shorter lead time and longer cutting tool life. The improved multi-swarm fruit fly optimisation algorithm provided better performance compared to traditional fruit fly optimisation algorithm and the commonly used genetic algorithm.

Further research will include generalising the optimisation approach to facilitate energy-efficient CNC machining for other types of operations such as turning, boring, and electro-discharge machining; and enhancing the robustness of the developed approach for online decision and optimisation.

ACKNOWLEDGEMENT

The authors would acknowledge Mr. G. Booth for the support and knowledge transferred during the machining experiments. The authors acknowledge the funding from the EU Smarter project (under the grant agreement PEOPLE-2013-IAPP-610675). MEF is grateful for funding from the Lloyd’s Register Foundation, a charitable foundation helping to protect life and property by supporting engineering-related education, public engagement and the application of research.

REFERENCES

[1] Shin S J, Woo J, Rachuri S (2017) Energy efficiency of milling machining: Component modeling and online optimization of cutting parameters. J Clean Prod 161:12–29

[2] Moreira L C, Li W D, Fitzpatrick M E, Lu X (2017) Research on energy consumption and energy efficiency of machine tools : a comprehensive survey. Int. J. Nanomanuf. Forthcoming issue (http://www.inderscience.com/info/ingeneral/forthcoming.php?jcode=IJNM)

[3] Yingjie Z (2014) Energy efficiency techniques in machining process: A review. Int J Adv Manuf Technol 71:1123–1132

[4] Peng T, Xu X (2012) The State of the Art in Energy Consumption Model – The Key to Sustainable Machining. Appl Mech Mater

232:592–599
[5] O'Driscoll E, O'Donnell G E (2013) Industrial power and energy metering e a state-of-the-art review. J Clean Prod 41:53–64
[6] Newman S T, Nassehi A, Imani-Asrai R, Dhokia V (2012) Energy efficient process planning for CNC machining. CIRP J Manuf Sci Technol 5:127–136
[7] Mori M, Fujishima M, Inamasu Y, Oda Y (2011) A study on energy efficiency improvement for machine tools. CIRP Ann Manuf Technol 60:145–148
[8] Diaz N, Redelsheimer E D D (2011) Energy Consumption Characterization and Reduction Strategies for Milling. Machine Tool Use Manuf Chem 82:22–24
[9] Kara S, Li W (2011) Unit process energy consumption models for material removal processes. CIRP Ann Manuf Technol 60:37–40
[10] Draganescu F, Gheorghe M, Doicin C V (2003) Models of machine tool efficiency and specific consumed energy. J Mater Process Technol 141:9–15
[11] Camposeco-Negrete C, de Dios C N J, Miranda-Valenzuela J C (2016) Optimization of cutting parameters to minimize energy consumption during turning of AISI 1018 steel at constant material removal rate using robust design. Int J Adv Manuf Technol 83:1341–1347
[12] Peng T, Xu X (2014) Energy-efficient machining systems: A critical review. Int J Adv Manuf Technol 72:1389–1406
[13] Lv J, Tang R, Jia S, Liu Y (2016) Experimental study on energy consumption of computer numerical control machine tools. J Clean Prod 112:3864–3874
[14] Liu Z Y, Guo Y B, Sealy M P, Liu Z Q (2016) Energy consumption and process sustainability of hard milling with tool wear progression. J Mater Process Technol 229:305–312
[15] Sealy M P, Liu Z Y, Zhang D, Guo Y B, Liu Z Q (2016) Energy consumption and modeling in precision hard milling. J Clean Prod 135:591–1601
[16] Moreira L C (2016) An Innovative Method for Process Planning for Sustainable Manufacturing. Dissertation, Coventry University
[17] Sonomez A I, Baykasoglu A, Dereli T, Filiz I H (1999) Dynamic optimization of multipass milling operations via geometric programming. Int J Mach Tools Manuf 39:297–320
[18] Wang S, Lu X, Li X X, Li W D (2015) A systematic approach of process planning and scheduling optimization for sustainable machining. J Clean Prod 87:914–929
[19] Ozcelik B, Oktem H, Kurtaran H (2005) Optimum surface roughness in end milling Inconel 718 by coupling neural network model and genetic algorithm. Int J Adv Manuf Technol 27:234–241
[20] Sreeram S, Kumar A S, Rahman M, Zaman M T (2006) Optimization of cutting parameters in micro end milling operations in dry cutting condition using genetic algorithms. Int J Adv Manuf Technol 30:1030–1039
[21] Li J G, Lu Y, Zhao H, Li P, Yao Y X (2014) Optimization of cutting parameters for energy saving. Int J Adv Manuf Technol 70:117–124
[22] Nee A Y C, Song B, Ong S-K, Peng T, Xu X (2013) A Universal Hybrid Energy Consumption Model for CNC Machining Systems. Re-engineering Manuf Sustain 251–256. https://doi.org/10.1007/978-981-4451-48-2_41
[23] Steel Express. EN24T Steel Properties. Available at: https://www.steelexpress.co.uk/engineeringsteel/EN24T-properties.html (Accessed: 30th January 2018)
[24] Lu X, Wang S, Li WD et al (2015) Development of a WSN based real time energy monitoring platform for industrial applications. IEEE 19th Int Conf Comput Support Coop Work Des 337–342
[25] Zhou L et al (2016) Energy consumption model and energy efficiency of machine tools: A comprehensive literature review. J Clean Prod 112:3721–3734
[26] Davim J P (2015) Traditional Machining Processes. Springer, London
[27] Xing B, Gao W (2014) Fruit fly optimization algorithm. In: Springer International Publishing (ed) Innovative Computational Intelligence: A Rough Guide to 134 Clever Algorithms, London, pp 167–170. https://doi.org/10.1007/978-3-319-03404-1_11
[28] Chen P-W, Lin W, Huang T, Pan WT (2013) Using fruit fly optimization algorithm optimized grey model neural network to perform satisfaction analysis for e-business service. Appl Math Inf Sci 7:459–465
[29] Pan, WT (2012) A new Fruit Fly Optimization Algorithm: Taking the financial distress model as an example. Knowledge-Based Syst 26:69–74
[30] Li H, Guo S, Li C, Sun J (2013) A hybrid annual power load forecasting model based on generalized regression neural network with fruit fly optimization algorithm. Knowledge-Based Syst 37:378–387
[31] Kanarachos S, Griffin J, Fitzpatrick M E (2017) Efficient truss optimization using the contrast-based fruit fly optimization algorithm. Comput Struct 182:137–148
[32] Yuan X, Dai X, Zhao J, He Q (2014) On a novel multi-swarm fruit fly optimization algorithm and its application. Appl Math Comput 233:260–271
[33] Yang X S (2014) Nature-inspired optimization algorithms. Elsevier